European Journal of Medicinal Chemistry 230 (2022) 114088

Contents lists available at ScienceDirect

European Journal of Medicinal Chemistry

journal homepage: http://www.elsevier.com/locate/ejmech

Efficient targeted oncogenic KRAS^{G12C} degradation via first reversible-covalent PROTAC

Fang Yang [1], Yalei Wen [1], Chaofan Wang, Yuee Zhou, Yang Zhou, Zhi-Min Zhang, Tongzheng Liu**, Xiaoyun Lu*

College of Pharmacy, Jinan University, 601 Huangpu Avenue West, Guangzhou, 510632, China

ARTICLE INFO

Article history:
Received 20 October 2021
Received in revised form
23 December 2021
Accepted 26 December 2021
Available online 3 January 2022

Keywords:
KRAS^{G12C}
Reversible-covalent inhibitors
PROTAC
Anticancer
Warheads

ABSTRACT

KRAS is the most frequently mutated oncogene and plays a predominant role in driving initiation and progression of multiple cancers. Attempts to degrade the oncogene KRAS^{G12C} with PROTAC strategy have been considered as an alternative strategy to combate cancers. However, the irreversible PROTACs may compromise the substoichiometric activity to decrease the potency. Herein, we report the development of YF135, the first reversible-covalent PROTAC capable of recruiting VHL mediated proteasomal degradation of KRAS^{G12C}. YF135 induces the rapid and sustained degradation of endogenous KRAS^{G12C} and attenuates pERK signaling in H358 and H23 cells in a reversible manner.

1. Introduction

The Kirsten rat sarcoma viral oncogene homologue (RAS) gene encodes a small GTPase enzyme that function as cellular signal transducers cycling between an inactive GDP-bound "off" state and active GTP-bound "on" state [1,2]. Among the three RAS isoforms (KRAS, HRAS and NRAS), KRAS is the most frequently mutated oncogene in human cancers with predominantly located at residues Glycine (G12/G13) and Glutamine (Q61) [3,4]. KRAS mutations attenuate GTPase activating proteins (GAPs) mediated enzymatic activity, leading to the accumulation of GTP-bound KRAS and hyperactivation of downstream signalling such as the RAS-RAF-MEK-ERK and the RAS-PI3K-AKT pathways and promoting cancer cell proliferation and survival [5,6]. Despite the well-recognized importance of oncogenic mutation of KRAS in cancers [7], the high binding affinity of the intrinsic ligand GTP for KRAS renders competitive inhibitors of GTP binding particularly challenging. Therefore, it has been referred to as an "undruggable" target in past decades [8,9]. KRAS^{G12C}, the most frequent KRAS mutation in lung cancer [10], can be targeted by small molecule inhibitors by forming a covalent bond with Cys12, providing an opportunity to target KRAS^{G12C} [11].

In 2013, Shokat and colleagues firstly developed the molecules specifically and covalently binding to the cysteine of KRAS^{G12C} with a "tethering" strategy [7]. This campaign finally led to the discovery of an orally bioavailable KRAS^{G12C} inhibitor ARS-1620 (**1**, Fig. 1) binding to a novel allosteric switch-II pocket (S-IIP) [12]. Followed this, AMG510 (**2**, Fig. 1) [13,14] and MRTX849 (**3**, Fig. 1) [15,16], developed by Amgen and Mirati Therapeutics, respectively, have showed promising efficacy against KRAS^{G12C} *in vitro* and *in vivo* and entered clinical studies. Particularly, AMG510 (Lumakras) has been approved by FDA as the first target therapy for lung cancer harboring KRAS^{G12C} mutation in 2021. Additionally, other two KRAS^{G12C} inhibitors ARS-3248 (JNJ-74699157, NCT04006301) and GDC-6036 (undisclosed structure, NCT04449874) are currently in clinical studies. However, the intrinsic and acquired resistance to these inhibitors has emerged in lung cancer harboring KRAS^{G12C} mutation [17,18]. Thus, chemical degradation of KRAS^{G12C} may provide an alternative therapeutic strategy for lung cancer.

Proteolysis-Targeting Chimeras (PROTACs) utilize heterobifunctional small molecules to tether a target protein and E3 ubiquitin ligase to form a ternary complex, enabling the E3 ligase to ubiquitinate the target protein and degrade it by 26S proteasome

* Corresponding author.
** Corresponding author.
E-mail addresses: liutongzheng@jnu.edu.cn (T. Liu), luxy2016@jnu.edu.cn (X. Lu).
[1] These authors contributed equally to this work.

https://doi.org/10.1016/j.ejmech.2021.114088
0223-5234/

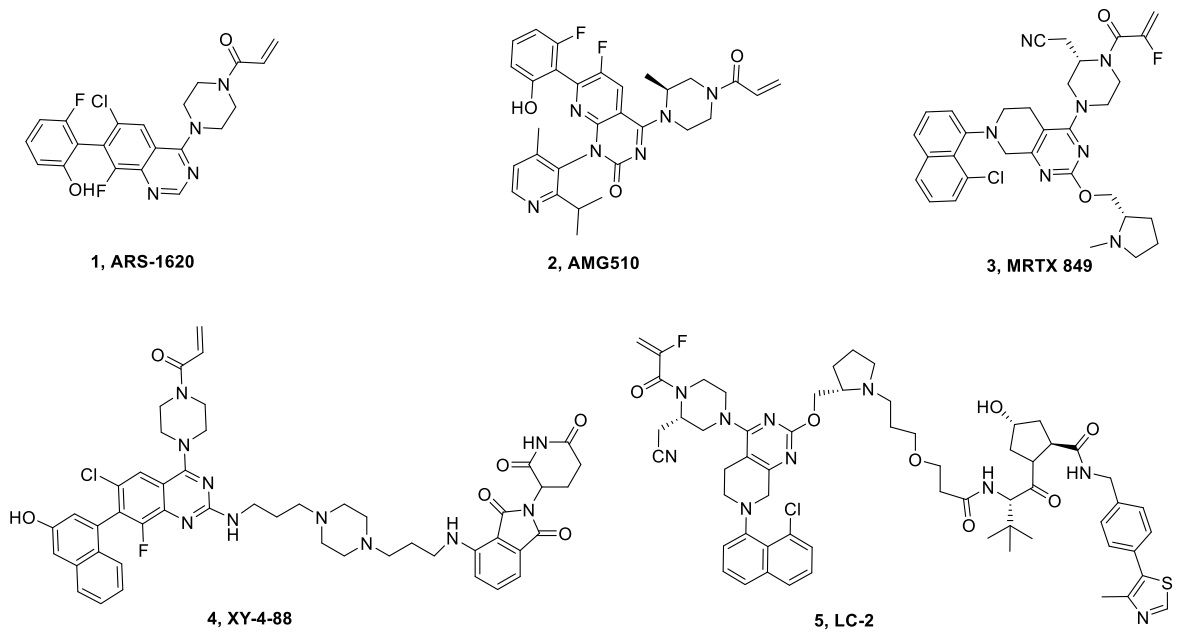

Fig. 1. The reported $KRAS^{G12C}$ inhibitors **1**–**3** and degraders **4**–**5**.

[19,20]. The first series of $KRAS^{G12C}$ PROTACs were reported based on an ARS-1620 analogue and the cereblon (CRBN) E3 ligase ligand pomalidomide by Gray's group [21]. The representative degrader XY-4-88 (**4**, Fig. 1) only showed the degradation in GFP-$KRAS^{G12C}$ reporter cells, but could not degrade endogenous $KRAS^{G12C}$ in pancreatic and lung cancer cells. Crew's group disclosed an endogenous $KRAS^{G12C}$ degrader LC-2 (**5**, Fig. 1) with the MRTX849 linkage VHL ligand [22,23]. LC-2 induced endogenous $KRAS^{G12C}$ degradation in a panel of cancer cell lines harbouring $KRAS^{G12C}$ at low concentrations e.g. 0.25—0.59 μM. LC-2 exhibited a reduced activity in degrading $KRAS^{G12C}$ because involved to engage $KRAS^{G12C}$ so-called "hook effects" at a high concentration (10 μM) [24]. Nevertheless, the irreversible bind mode of PROTACs may compromise the substoichiometric activity of PROTACs to decrease the potency [25,26]. Thus, we hoped that reversible-covalent PROTAC may have the potential to avoid this defect and enhance potency in degradation of $KRAS^{G12C}$ [24,27]. Herein, we reported the first cyanacrylamide-based reversible-covalent PROTAC **YF135** designed based on the scaffold of MRTX849 linkage VHL ligand (Fig. 2). **YF135** induced the rapid and sustained endogenous $KRAS^{G12C}$ degradation by recruiting VHL mediated proteasomal degradation mechanism in a reversible manner and suppressed p-ERK in H358 and H23 cell lines.

2. Chemistry

The synthesis of **6a**-**6e** is summarized in Scheme 1. Directly nucleophilic reaction with available *tert*-butyl 2,4-dichloro-5,8-dihydropyrido[3,4-d]pyrimidine-7(6H)-carboxylate **7** and benzyl (*S*)-2-(cyanomethyl)piperazine-1-carboxylate obtained intermediate **8**. Coupling of **8** and *N*-methyl-*L*-prolinol using $Pd(OAc)_2$ as catalyst gave **9**, which followed by deprotection and Buchwald-Hartwig cross coupling reaction with 1-bromo-8-chloronaphthalene yielded the key intermediate **10**. Further deprotection of **10** under Pd/C and H_2 atmosphere and condensation with cyanoacetic acid obtained **11**. Addition of **11** with various aliphatic aldehydes gave the desired derivatives **6a**-**6e**.

Reagents and conditions: (a) MeCN, Et_3N, 60 °C, 3h, 72%; (b) PhMe, $Pd(OAc)_2$, BINAP, Cs_2CO_3, 110 °C, 10h, 52%; (c) (i) DCM, TFA, rt, 3h, (ii) PhMe, 1-bromo-8-chloronaphthalene, $Pd_2(dba)_3$, XantPhos, Cs_2CO_3, 110 °C, 12h, 48% for two steps; (d) (i) MeOH, Pd/C, H_2, rt, 2h, (ii) DCM, cyanoacetic acid, HATU, Et_3N, rt, 1h, 21% for two steps; (e) DCM, piperidine, rt, 11—27%.

The synthetic procedure of degrader **YF135** is described in Scheme 2. Cyclization of commercial available materials **12** and 2-methyl-2-thiopseudourea sulfate gave intermediate **13**, followed by reaction with Tf_2O obtained **14**. Coupling with benzyl (*S*)-2-cyanomethylpiperazine-1-carboxylate **15** gave compound **16**, followed by deprotection and Buchwald-Hartwig Cross Coupling reaction with 1-bromo-8-chloronaphthalene led to the key intermediate **17**. Oxidation of **17** by m-CPBA, then substitution with *tert*-butyl (*S*)-3-(3-(2-(hydroxymethyl)pyrrolidin-1-yl)propoxy) propanoate **18** (Supporting information, Scheme S1) obtained **19** as white solid. Deprotection of **19** under Pd/C catalysis obtained **20**, which further condensation with 2-cyano-3-cyclopropylacrylic acid **21** afforded intermediate **22**. Finally, deprotection of **22** and then condensation with the VHL ligand **23** afforded the desired degrader **YF135**.

Reagents and conditions: (a) MeOH, NaOMe, 2-methyl-2-thiopseudourea sulfate, rt, overnight, 64%; (b) CH_2Cl_2, Tf_2O, DIPEA, 0 °C-rt, 16h, 44%; (c) MeCN, DIPEA, 100 °C, N_2, 3h, 80%; (d) (i) DCM, TFA, rt, 3h, (ii) PhMe, 1-bromo-8-chloronaphthalene, $Pd_2(dba)_3$, XantPhos, Cs_2CO_3, 100 °C, 18h, 56% for two steps; (e) (i) DCM, *m*-CPBA, rt, overnight, 46%; (ii) PhMe, *tert*-butyl (*S*)-3-(3-(2-(hydroxymethyl)pyrrolidin-1-yl)propoxy)propanoate, *t*-BuONa, rt, 2h, 22%; (f) MeOH, DCM, Pd/C, H_2, rt, 36h, 52%; (g) DCM, 2-cyano-3-cyclopropylacrylic acid, HATU, Et_3N, rt, 1h, 27%; (h) (i) DCM, TFA, rt, 0.5h, (ii) DMF, VHL ligand, HATU, Et_3N, rt, 2h, 22% for two steps.

3. Results and discussion

Cyanoacrylamide-based electrophile has been widely used as an effective reversible-covalent warhead in recent years [28,29]. Thus, a series of cyanoacrylamide-based warheads were introduced to the piperazine part of MRTX849 instead of original acrylamide with structure-based design (Fig. 2A), as Cys12 is located outside the

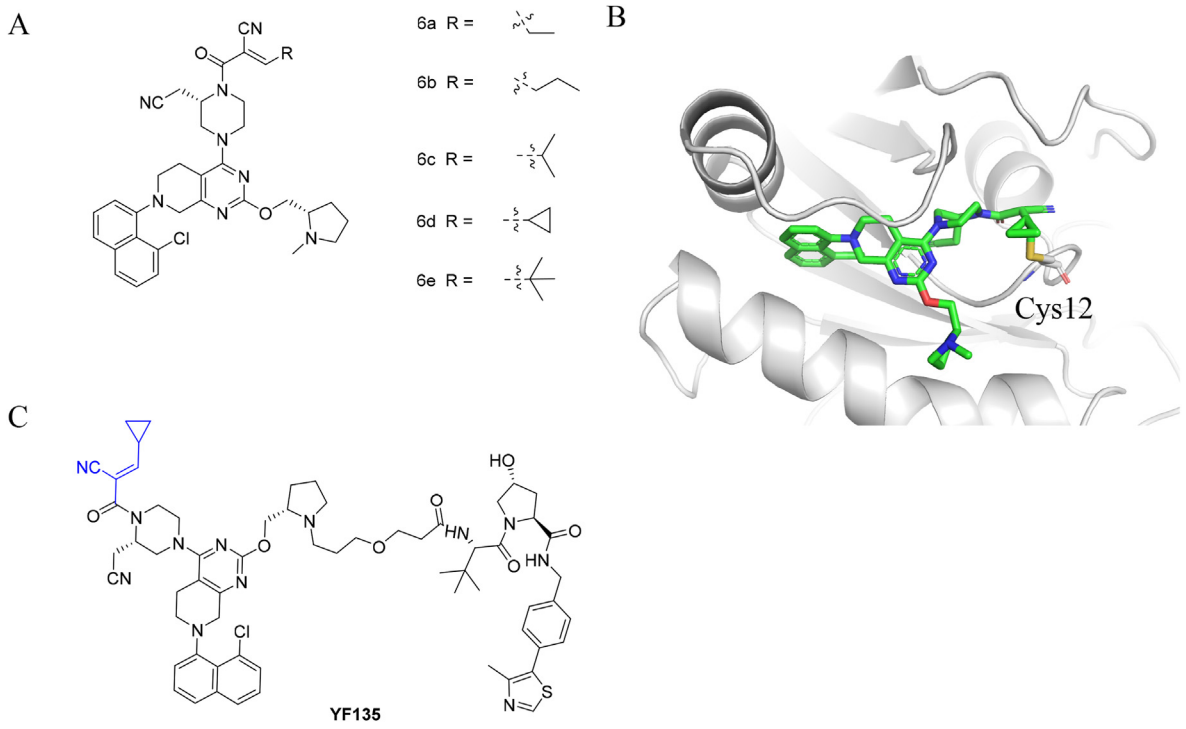

Fig. 2. The rational drug design of reversible-covalent KRAS^{G12C} PROTACs. (A) The designed cyanoacrylamide-based analogues of MRTX849. (B) The predicted binding mode of **6d** (green) with KRAS^{G12C}. (C) The chemical structure of designed PROTAC **YF135**.

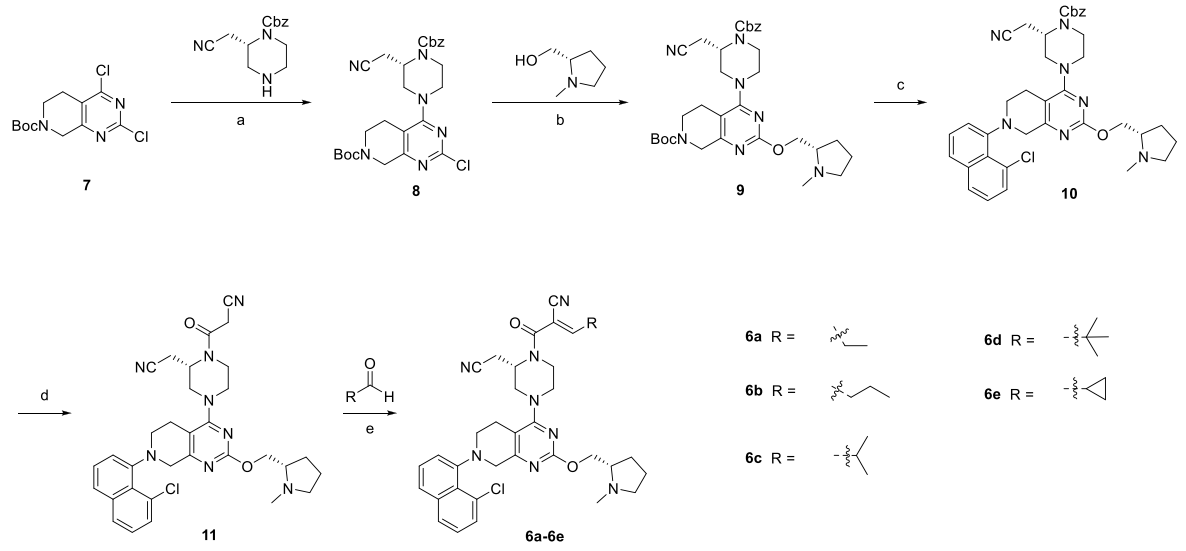

Scheme 1. Synthesis of **6a-6e.**

allosteric S-IIP to accommodate the electrophile branched-alkyl capping groups (Fig. 2B). The resulting compounds **6a-6e** were synthesized and evaluated their inhibitory activity against KRAS^{G12C} by HTRF assay [30]. Among them, compound **6d** exhibited the most potent activity against KRAS^{G12C} with an IC_{50} value of 25.44 nM (Table 1). While other compounds **6a-6c** and **6e** exhibited the less potency against KRAS^{G12C}compared to **6d** with IC_{50} values of 96.32–639.91 nM. The anti-proliferative activities of compounds **6a-6e** against H358, H23 and A549 cells were evaluated by CCK-8 assay using AMG510 as a positive control. As showed in Table 2, these compounds displayed anti-proliferative activities with IC_{50} values in micromolar range. It was indicated that the inhibitory activities were decreased with the increased or decreased volume of branched-alkyl capping groups in the cyanoacrylamide group (Table 2). We hypothesized that the relatively low level of conformational flexibility of Cys12 in the entrance of pocket may limit the geometry and size of the electrophilic warheads. Molecular docking studies showed that **6d** occupies the allosteric S-IIP of KRAS^{G12C} with a similar binding mode to that of MRTX849 (pdb: 6UT0). The cluster docking conformation of **6d** was showed in Fig. S1. Cyanoacrylamide formed a covalent-bond with Cys12 in a *trans* configuration and the methylpyrrole group was exposed to solvent

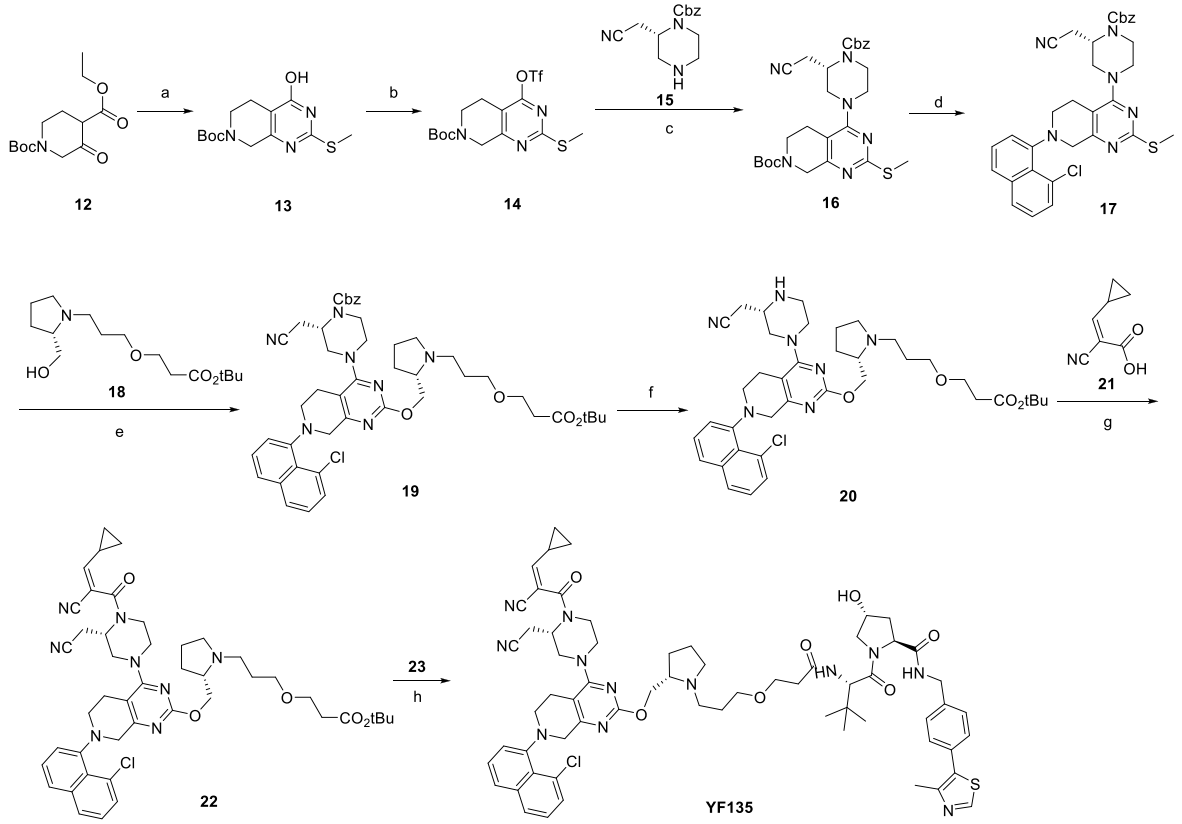

Scheme 2. Synthesis of **YF135.**

Table 1
The inhibitory activities of **6a**-**6e** against $KRAS^{G12C}$.

Compds	6a	6b	6c	6d	6e	AMG510
IC_{50} (nM)[a]	96.32 ± 0.01	270.88 ± 0.03	283.84 ± 0.006	25.44 ± 0.003	639.91 ± 0.1	9.66 ± 0.02

[a] IC_{50} value were represents mean from two independent experiment.

Table 2
The anti-proliferative activity of **6a**-**6e** against H358, H23 and A549 cells.

Compds	IC_{50} (μM)[a]		
	H358	H23	A549
6a	5.13	9.55	8.20
6b	13.41	7.40	25.32
6c	13.67	3.15	>50
6d	4.7	5.25	13.27
6e	0.796	6.33	16.14
AMG510	8.4 nM	111.5 nM	>50

[a] IC_{50} were calculated from three independent experiments.

region, which was suitable for linkage an E3 ligase ligand for PROTACs design (Fig. 2B).

To investigate the binding mode of **6d** with $KRAS^{G12C}$, Matrix-Assisted Laser Desorption/Ionization Time of Flight Mass Spectrometry (MALDI-TOF-MS) study was performed. As showed in Fig. 3, the molecular weight measured *m*/*z* of 20003 Da is consistent with the sum of the molecular weight of **6d** (M = 650.28) and $KRAS^{G12C}$ (M = 19353 Da) after incubation for 2hrs. Meanwhile, the dialysis assay demonstrated partly restoration of $KRAS^{G12C}$ after 24hrs with the molecular weight as 19353 Da. These results showed that **6d** could bind $KRAS^{G12C}$ in a reversible-covalent

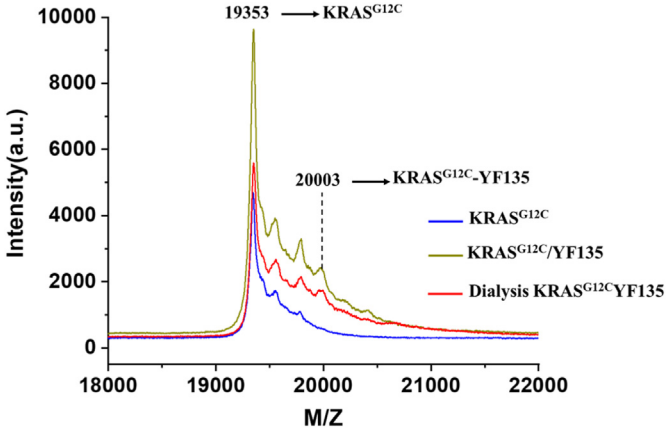

Fig. 3. MALDI-TOF MS determination of the $KRAS^{G12C}$ and **6d**. The blue line indicates the molecular weight of $KRAS^{G12C}$ (19353Da); The light green line indicates the sum of the molecular weight of **6d** (M = 650.28) and $KRAS^{G12C}$ (20003Da), The red line indicates the partial restoration of $KRAS^{G12C}$ after the dialysis of **6d**.

binding mode and serve as a cyanacrylamide-based reversible-covalent warhead to design PROTAC. Thus, **YF135** was subsequently synthesized by tethering **6d** as the $KRAS^{G12C}$ ligand, VHL as a ligase

ligand and ethylenedioxy as a linker to explore the degradation ability (Fig. 2C).

We first tested the anti-proliferative effects of **YF135** on lung cancer cell lines H358 and H23 harboring KRAS^{G12C} mutation, and A549 harboring KRAS^{G12S} mutation. AMG510 was used as a positive control. As showed in Fig. 4, **YF135** inhibited the proliferation of H358 and H23 cells with IC_{50} values of 153.9 and 243.9 nM, respectively, while no obvious inhibition was observed in A549 cells harboring KRAS^{G12S} mutations. These results indicated that **YF135** possessed the inhibitory selectivity against KRAS^{G12C} mutation, which is similar to that of AMG510.

We next measured the degradation effect of **YF135** on KRAS^{G12C} in H358 and H23 cells. We found that the treatment of **YF135** in H358 and H23 cells could obviously decrease the protein level of KRAS^{G12C} and phospho-ERK in a time dependent manner, while the protein level of total ERK was not affected (Fig. 5A). The treatment of YF135 at 3 μM for 16 h reduced the KRAS^{G12C} protein level substantially, and the maximum effect was observed at 24 h. As showed in Fig. 5B and 5C, **YF135** decreased the level of KRAS^{G12C} and phospho-ERK in a dose-dependent manner with DC_{50} values of 3.61 and 1.68 μM in H358 cells, respectively. In H23 cells, it also dose-dependently decreased the level of KRAS^{G12C} and phospho-ERK with DC_{50} values of 4.53 and 1.44 μM, respectively. However, no effects on either KRAS protein level or phospho-ERK were observed in A549 cells harboring KRAS^{G12S} mutation (Fig. 5D). Furthermore, we also treated H358 cells with **YF135** at 10 μM, 20 μM and 30 μM, while no obvious "hook effects" were observed (Fig. 5E). These results indicated that **YF135** is an effective and selective KRAS^{G12C} degradation agent.

The ubiquitin-proteasome system is one major intracellular pathway for protein degradation [31,32]. We next investigated the contribution of proteasome in **YF135**-induced KRAS^{G12C} degradation. As showed in Fig. 6A, the proteasome inhibitor MG-132 can significantly rescue **YF135** induced decrease of KRAS protein level and phosphor-ERK in H358 and H23 cells. In order to determine whether **YF135** is a reversible-covalent PROTAC, the washout assay was performed in H358 and H23 cells. As showed in Fig. 6B, the treatment of **YF135** in H358 cells for 24hrs induced the significant degradation on KRAS^{G12C} and decreased the level of phospho-ERK, while the washout by fresh medium at different time points (8, 12 and 16hrs) significantly rescued such effects of **YF135** on KRAS^{G12C} protein and phospho-ERK. Next, cycloheximide (CHX), a protein synthesis inhibitor, was used to exclude the involvement of the re-synthesis of KRAS^{G12C} in cells. As showed in Fig. 6C, the treatment of CHX decreased the protein level of KRAS^{G12C} in H358 cells. We found that the combination of CHX and **YF135** could further reduce it, while the washout by fresh medium could at least partially rescue such effects. These results demonstrated that **YF135** could induce the degradation of KRAS^{G12C} in a reversible manner.

To further verify the mechanism of action of degradation, E3 ligase ligand (VH-032) and **6d** were performed in a rescue assay. As showed in Fig. 6D and 6E, VH-032 and **6d** could compete with YF135 and decrease its effect on the degradation of KRAS^{G12C}. These results indicated that YF135 induces degradation of KRAS^{G12C} through the E3 ligase VHL mediated proteasome pathway. The molecular modelling also suggested that **YF135** covalently bound to KRAS^{G12C} and VHL ligase to form a ternary complex (Fig. 7).

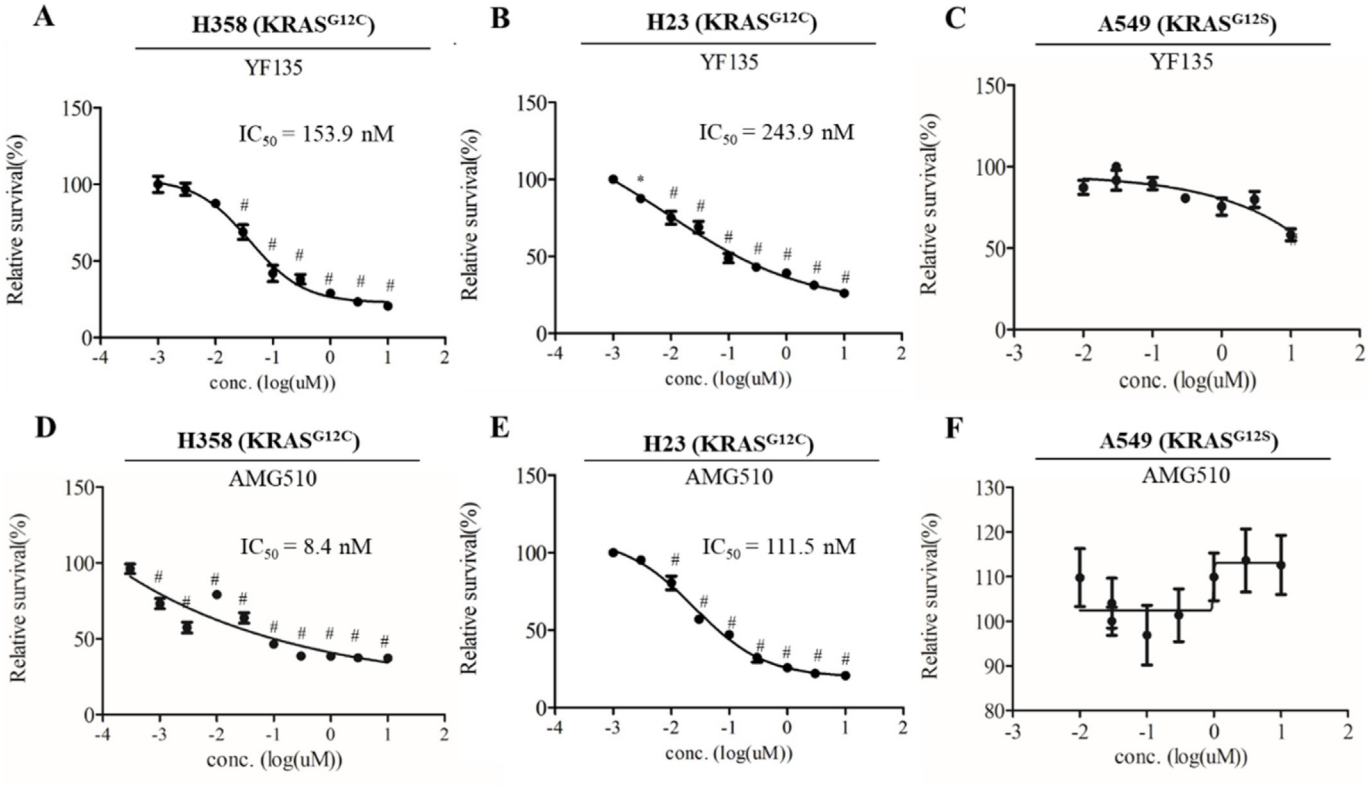

Fig. 4. Compound YF135 inhibited the proliferation of cells harboring KRAS^{G12C}, but not KRAS^{G12S}. H358 and H23 cells harboring KRAS^{G12C} mutation were treated with various concentration of YF135 (**A**, **B**) and AMG510 (**D**, **E**), respectively. A549 cells harboring KRAS^{G12S} mutation were treated with various concentration of YF135 (**C**) and AMG510 (**F**), respectively. The proliferation of cells were measured by CCK8 assay. Quantified data represents mean ± SD from four independent replicates. **p < 0.01; #p < 0.001 when compared with the DMSO group. Statistical analysis was performed using One-way ANOVA.

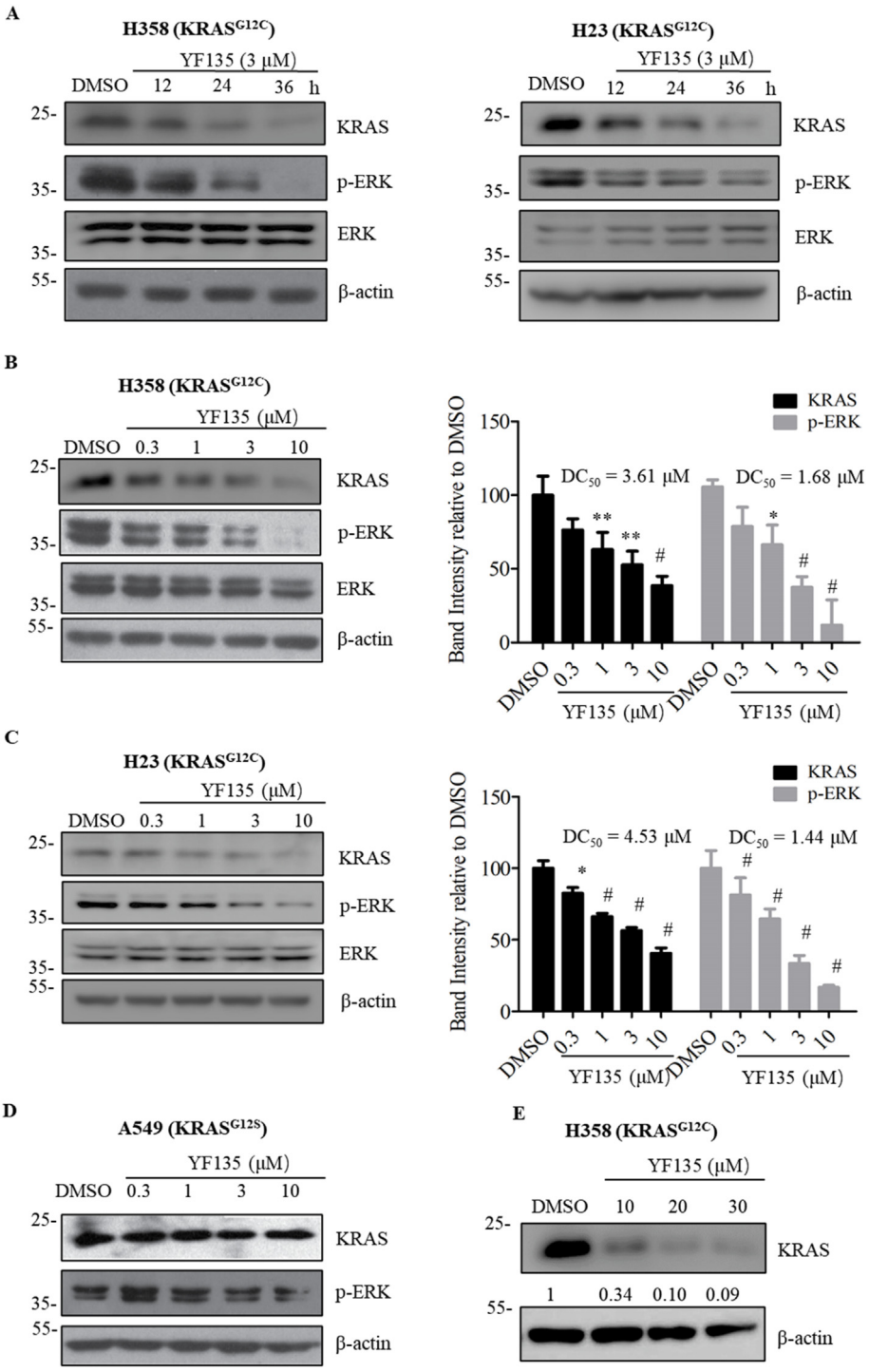

Fig. 5. YF135 degraded endogenous KRAS in $KRAS^{G12C}$-mutant cells. (**A**) Time-dependent degradation $KRAS^{G12C}$ by YF135 at 3 μM in H358 and H23 cells. (**B** and **C**) Dose-dependent degradation of $KRAS^{G12C}$ by YF135 for 24hrs in H358 and H23 cells. (**D**) Dose-course studies of degradation by YF135 for 24hrs in A549 cells. (**E**) Dose-dependent degradation of $KRAS^{G12C}$ by YF135 at high concentrations (10, 20 and 30 μM). The protein levels of KRAS and p-ERK were determined by western blotting. Quantified data represents mean ± SD from four independent replicates. Not Significant (N.S.); $^{**}p < 0.01$; $^{\#}p < 0.001$ when compared with the DMSO group, and statistical analysis was performed using One-way ANOVA.

4. Conclusion

In conclusion, we introduced a series of cyanoacrylamide-based warheads to the scaffold of MRTX849 and obtained **6d** as a $KRAS^{G12C}$ inhibitor with an IC_{50} values of 25.44 nM. Protein mass spectrometry results showed **6d** could bind to $KRAS^{G12C}$ in a reversible-covalent manner. The first reversible-covalent PROTAC **YF135** was designed and synthesized by tethering **6d** as the $KRAS^{G12C}$ ligand, VHL as a ligase ligand and ethylenedioxy as a linker. **YF135** could significantly induce the degradation of $KRAS^{G12C}$ and consequently decrease phospho-ERK level in H358 and H23 cells. The degradation effect of **YF135** on $KRAS^{G12C}$ was

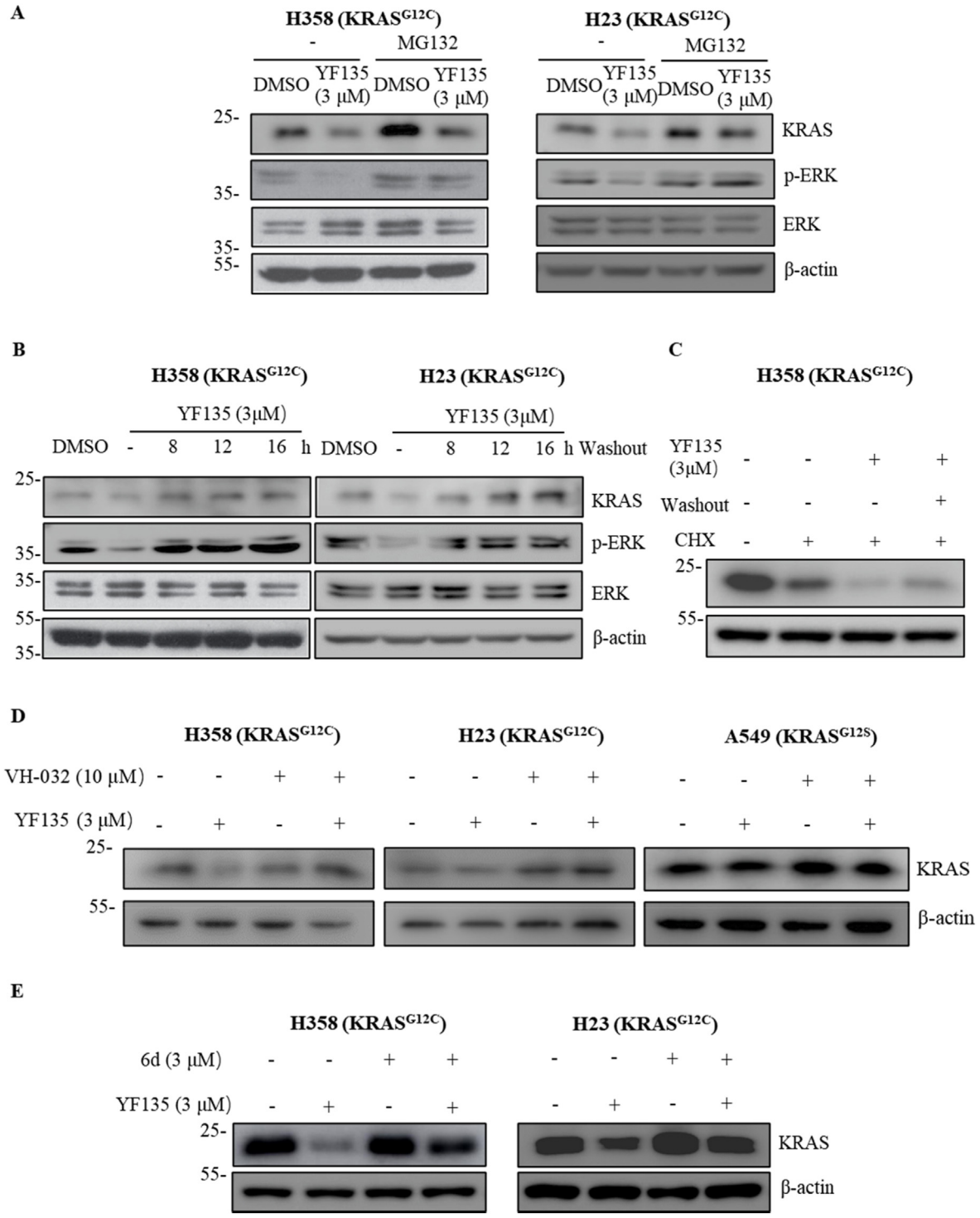

Fig. 6. Mechanism studies of PROTAC YF135 in H358 and H23 cells using Western blotting. (**A**) YF135 mediated KRAS^{G12C} degradation is rescued by the proteasome inhibitor MG132. (**B**-**C**) YF135 mediated KRAS^{G12C} degradation is reversible in the absence (B) or presence (C) of cycloheximide (CHX). (**D**) YF135 mediated KRAS^{G12C} degradation is rescued by the E3 ligase ligand (VH-032). (**E**) YF135 mediated KRAS^{G12C} degradation is rescued by the ligand 6d.

identified through E3 ligase VHL mediated proteasome pathway. The degradation activity of **YF135** is less potent than LC-2, which is possibly due to the decreased binding affinity of **6d** to KRAS^{G12C}. Collectively, compound **YF135** could be utilized as a lead molecule for the development of new KRAS^{G12C} degrader based therapy.

5. Experimental section for chemistry

5.1. Chemistry

General Methods: Unless otherwise noted, all solvents and reagents were obtained from commercial and used without further purifications. MRTX849 and AMG510 was purchased from Target

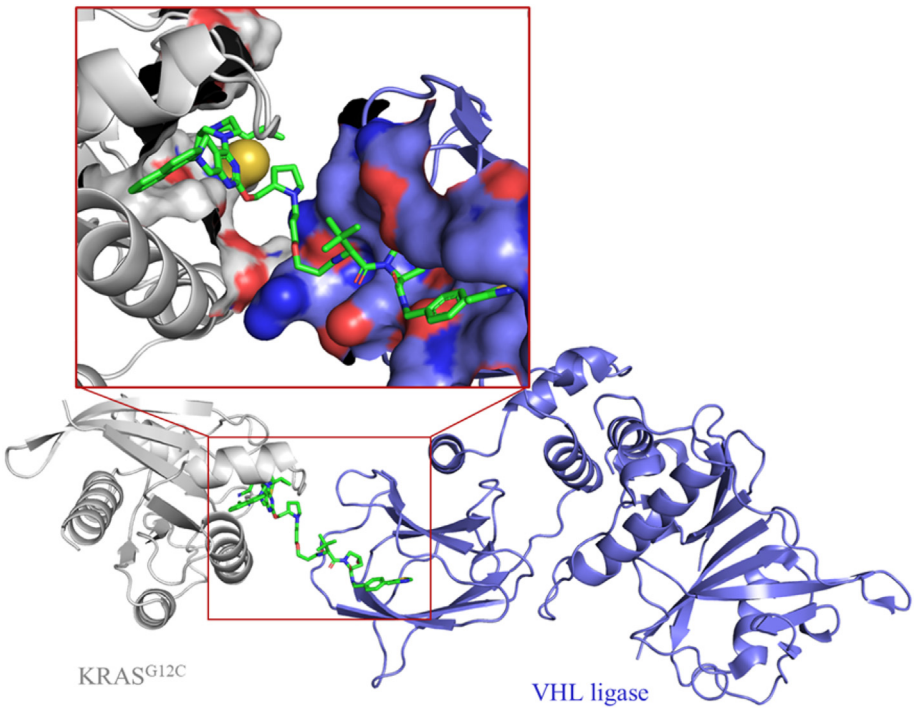

Fig. 7. The predicted binding mode of YF135 with KRAS^{G12C} and VHL ligase as a ternary complex. The KRAS^{G12C} protein, VHL ligase and YF135 were coloured as gray, blue and green, respectively.

Molecule Corp, High resolution ESI-MS was performed on an Agilent 1100 HPLC/MS system. ^{1}HNMR and ^{13}CNMR spectra were recorded on a Bruker AVANCE AV-400/600 spectrometer (Bruker Company, Germany) at 400 MHz and 151 MHz, respectively. They were recorded in DMSO-d_6, $CDCl_3$ and Acetone-d_6. Chemical shifts (d) of NMR are reported in parts per million (ppm) units relative to internal control (TMS) and Coupling constants (J) are expressed in hertz (Hz). All reactions were monitored by TLC plates purchased from Qingdao Haiyang Chemical Ltd, China, and fluorescent indicator visualizable at 254 nm and 365 nm. Flash chromatography separations were obtained on Silica Gel (300–400 mesh) using dichloromethane/methanol or Petroleum ether/ethyl acetate as eluents.

5.1.1. Synthesis of 6a-6e

5.1.1.1. tert-butyl (S)-4-(4-((benzyloxy)carbonyl)-3-(cyanomethyl) piperazin-1-yl)-2-chloro-5,8-dihydropyrido[3,4-d]pyrimidine-7(6H)-carboxylate (8). To a solution of *tert*-butyl 2,4-dichloro-5,8-dihydropyrido[3,4-d]pyrimidine-7(6H)-carboxylate **7** (5.0 g, 16.4 mmol, 1.0 eq.) in MeCN (50.0 mL) was added TEA (3.3 g, 2.0 eq.) followed by benzyl (*S*)-2-(cyanomethyl)piperazine-1-carboxylate (4.5 g, 1.05 eq.), The mixture was stirred at 60 °C for 3h. Then, solvent was removed under vacuum after TLC showed the reagent completely consumption, The residue was purified by column chromatography (SiO_2, PE/EA = 10:1 to 5:1) to give title compound (6.2 g, 72% yield) as white solid. ^{1}H NMR (400 MHz, $CDCl_3$) δ 7.43–7.37 (m, 5H), 5.21 (s, 2H), 4.70–4.65 (m, 2H), 4.46 (d, J = 16.0 Hz, 1H), 4.15–4.07 (m, 2H), 3.91–3.83 (m, 2H), 3.42–3.39 (m, 3H), 3.12 (t, J = 12.0 Hz, 1H), 2.83–2.75 (m, 1H), 2.71–2.66 (m, 3H), 1.50 (s, 9H). ESI-MS m/z: 527.3 $[M+H]^+$.

5.1.1.2. tert-butyl 4-((S)-4-((benzyloxy)carbonyl)-3-(cyanomethyl) piperazin-1-yl)-2-(((S)-1-methylpyrrolidin-2-yl)methoxy)-5,8-dihydropyrido[3,4-d]pyrimidine-7(6H)-carboxylate (9). To a mixture of **8** (6.0 g, 11.4 mmol, 1.0 eq.) in toluene (250.0 mL) was added *N*-methyl-*L*-prolinol (1.38 g, 1.05 eq.), $Pd(OAc)_2$ (250.0 mg, 0.01 eq.), BINAP (665.0 mg, 0.02 equiv.) and Cs_2CO_3 (11.1 g, 3.0 eq.). The reaction mixture was stirred at 110 °C for 10 h under an atmosphere of nitrogen. The mixture was filtered and organic layer was concentrated, dried and purified by column chromatography (SiO_2, DCM/MeOH = 20:0 to 20:1) to afford **9** (3.59 g, 52% yield) as a white solid.

^{1}H NMR (400 MHz, $CDCl_3$) δ 7.44–7.35 (m, 5H), 5.20 (s, 2H), 4.66–4.59 (m, 2H), 4.38–4.34 (m, 2H), 4.16–4.12 (m, 2H), 3.97 (d, J = 12.0 Hz, 1H), 3.81 (d, J = 12.0 Hz, 1H), 3.35–3.27 (m, 3H), 3.09 (t, J = 8.0 Hz, 1H), 2.99 (t, J = 12.0 Hz, 1H), 2.84–2.78 (m, 1H), 2.73 (d, J = 8.0 Hz, 1H), 2.69–2.58 (m, 3H), 2.48 (s, 3H), 2.88 (dd, J_1 = 6.0 Hz, J_2 = 18.0 Hz, 1H), 2.09–1.96 (m, 2H), 1.86–1.69 (m, 3H), 1.50 (s, 9H). ESI-MS m/z: 606.3 $[M+H]^+$.

5.1.1.3. benzyl (S)-4-(7-(8-chloronaphthalen-1-yl)-2-(((S)-1-methylpyrrolidin-2-yl)methoxy)-5,6,7,8-tetrahydropyrido[3,4-d]pyrimidin-4-yl)-2-(cyanomethyl)piperazine-1-carboxylate (10). To a solution of **9** (3.59 g, 5.9 mmol, 1.0 eq.) in DCM (25 mL), was added TFA (15.0 mL) and the mixture was stirred at 20 °C for 3 h. The reaction mixture was quenched with saturated $NaHCO_3$ solution, extracted with DCM (3 x 50 mL) and the organic layer was dried under vacuum to give a yellow solid (2.5 g, 4.9 mmol, 83.3% Yield) which was used for the next step immediately without further purification. ESI-MS m/z: 506.3 $[M+H]^+$.

To a solution of above product (2.5 g, 4.9 mmol, 1.0 eq.) and 1-bromo-8-chloronaphthalene (1.2 g, 5.1 mmol, 1.04 eq.) in toluene (50.0 mL) was added $Pd_2(dba)_3$ (450 mg, 0.1 eq.), XantPhos (430.0 mg, 0.15 eq.) and Cs_2CO_3 (4.8 g, 3.0 eq.). The mixture was stirred at 110 °C for 12 h under an atmosphere of nitrogen. The mixture was filtered, and organic layer was concentrated, dried and purified by column chromatography (SiO_2, DCM/MeOH = 10:0 to 10:1) to afford **10** (1.8 g, 54.8% yield) as a brown solid. ^{1}H NMR (400 MHz, $CDCl_3$) δ 7.76 (d, J = 8.0 Hz, 1H), 7.61 (d, J = 8.0 Hz, 1H), 7.53 (d, J = 8.0 Hz, 1H), 7.44 (t, J = 8.0 Hz, 1H), 7.40–7.39 (m, 5H),

7.34 (t, J = 8.0 Hz, 1H), 7.23 (d, J = 8.0 Hz, 1H), 5.19 (s, 2H), 4.45–4.37 (m, 2H), 4.18–1.44 (m, 1H), 3.86 (d, J = 20.0 Hz, 1H), 3.72–3.66 (m, 2H), 3.63–3.55 (m, 5H), 3.47–3.41 (m, 2H), 3.16–3.08 (m, 3H), 2.71–2.66 (m, 1H), 2.48 (s, 3H), 2.28 (dd, J_1 = 8.0 Hz, J_2 = 16.0 Hz, 1H), 2.10–2.04 (m, 3H), 1.87–1.72 (m, 3H). ESI-MS m/z: 666.3 $[M+H]^+$.

5.1.1.4. 3-((S)-4-(7-(8-chloronaphthalen-1-yl)-2-(((S)-1-methylpyrrolidin-2-yl)methoxy)-5,6,7,8-tetrahydropyrido[3,4-d]pyrimidin-4-yl)-2-(cyanomethyl)piperazin-1-yl)-3-oxopropanenitrile (11). To a solution of **10** (1.8 g, 2.7 mmol, 1.0 eq.) in MeOH (50.0 mL) was added DCM (5.0 mL) and Pd/C (0.2 g, 10 wt %) under an atmosphere of nitrogen. The vessel was purged several times by alternating a vacuum and backfilling with hydrogen gas. The mixture was stirred at room temperature overnight. Then, filtered and concentrated under reduced pressure to give a brown solid (0.9 g, 62.5% yield) which was used for the next step immediately without further purification. ESI-MS m/z: 532.3 $[M+H]^+$.

To a solution of above product (0.5 g, 0.94 mmol, 1.0 eq.) and Cyanoacetic acid (104.0 mg, 1.3 eq.) in DCM (20.0 mL) was added HATU (464.0 mg, 1.3 eq.) and TEA (190.0 mg, 2.0 eq.). The mixture was stirred at room temperature for 1 h under an atmosphere of nitrogen. Then, dried and purified by column chromatography (SiO_2, DCM/MeOH = 20:0 to 20:1) to afford **11** (250.0 mg, 45% yield) as a brown solid. ^{1}H NMR (400 MHz, $CDCl_3$) δ 7.77 (d, J = 8.0 Hz, 1H), 6.62 (t, J = 8.0 Hz, 1H), 7.54 (d, J = 8.0 Hz, 1H), 7.49–7.43 (m, 1H), 7.35 (t, J = 8.0 Hz, 1H), 7.24 (dd, J_1 = 8.0 Hz, J_2 = 20.0 Hz, 1H), 7.49–7.38 (m, 2H), 4.47–4.38 (m, 2H), 4.22–4.06 (m, 2H), 3.93–3.85 (m, 1H), 3.81–3.76 (m, 1H), 3.73–3.67 (m, 1H), 3.62–3.57 (m, 2H), 3.45 (dd, J_1 = 4.0 Hz, J_2 = 16.0 Hz, 1H), 3.28–3.17 (m, 2H), 3.11 (d, J = 12.0 Hz, 2H), 2.99 (dd, J_1 = 8.0 Hz, J_2 = 16.0 Hz, 1H), 2.88–2.82 (m, 1H), 2.77 (dd, J_1 = 8.0 Hz, J_2 = 16.0 Hz, 1H), 2.72–2.69 (m, 1H), 2.62–2.59 (m, 1H), 2.50 (s, 3H), 2.35–2.28 (m, 1H), 2.11–2.02 (m, 3H), 1.87–1.74 (m, 3H). ESI-MS m/z: 599.3 $[M+H]^+$.

5.1.1.5. (E/Z)-2-((S)-4-(7-(8-chloronaphthalen-1-yl)-2-(((S)-1-methylpyrrolidin-2-yl)methoxy)-5,6,7,8-tetrahydropyrido[3,4-d]pyrimidin-4-yl)-2-(cyanomethyl)piperazine-1-carbonyl)but-2-enenitrile (6a). A 25 mL vial bearing a magnetic stir bar was charged with the **11** (100.0 mg, 0.17 mmol, 1.0 eq.), acetaldehyde (40% in water, 11.0 mg, 1.5 eq.), piperidine (1.5 mg, 0.1 eq.) and DCM (5.0 mL), The reaction mixture was stirred at room temperature for 2.5 h. The reaction mixture was concentrated under reduced pressure and the resulting residue was purified by column chromatography (SiO_2, DCM/MeOH = 20:0 to 20:1) to afford product (15.5 mg, 15.0% yield) as white solid. ^{1}H NMR (400 MHz, $CDCl_3$ mixture of rotamers): δ 7.77 (d, J = 8.0 Hz, 1H), 7.63 (t, J = 8.0 Hz, 1H), 7.54 (d, J = 8.0 Hz, 1H), 7.49–7.43 (m, 1H), 7.36–7.34 (m, 2H), 7.24 (dd, J_1 = 4.0 Hz, J_2 = 20.0 Hz, 1H), 4.94 (br, 1H), 4.47–4.41 (m, 2H), 4.20–4.15 (m, 2H), 4.07 (d, J = 8.0 Hz, 1H), 3.95–3.83 (m, 2H), 3.62–3.59 (m, 1H), 3.50–3.45 (m, 1H), 3.26–3.18 (m, 2H), 3.16–3.10 (m, 3H), 2.84–2.81 (m, 1H), 2.70 (br, 1H), 2.58 (t, J = 8.0 Hz, 1H), 2.50 (s, 3H), 2.31–2.29 (m, 1H), 2.24 (d, J = 4.0 Hz, 3H), 2.10–2.04 (m, 1H), 1.89–1.84 (m, 2H), 1.78–1.77 (d, J = 4.0 Hz, 2H).^{13}C NMR (151 MHz, $CDCl_3$) δ 166.37, 166.25, 162.75, 162.71, 148.43, 148.11, 137.34, 130.07, 129.72, 128.25, 126.43, 126.01, 125.94, 125.65, 125.16, 125.03, 118.75, 118.63, 109.20, 69.84, 64.02, 59.01, 58.69, 57.63, 53.44, 50.38, 47.79, 47.41, 41.72, 29.06, 26.15, 25.57, 22.97, 17.82. HR-MS (ESI+) calcd for $C_{34}H_{37}ClN_8O_2$ $[M+H]^+$ 625.2728, found 625.2770.

5.1.1.6. (E/Z)-2-((S)-4-(7-(8-chloronaphthalen-1-yl)-2-(((S)-1-methylpyrrolidin-2-yl)methoxy)-5,6,7,8-tetrahydropyrido[3,4-d]pyrimidin-4-yl)-2-(cyanomethyl)piperazine-1-carbonyl)pent-2-enenitrile (6b). Synthesized according to the method of **6a** using propionaldehyde in place of Acetaldehyde to afford product **6b** (12.0 mg, 0.019 mmol, 16% yield) as white solid. ^{1}H NMR (400 MHz, $CDCl_3$ mixture of rotamers): δ 7.77 (d, J = 4.0 Hz, 1H), 7.64 (t, J = 6.0 Hz, 1H), 7.54 (d, J = 4.0 Hz, 1H), 7.49–7.41 (m, 2H), 7.35 (t, J = 6.0 Hz, 1H), 7.24 (dd, J_1 = 4.0 Hz, J_2 = 16.0 Hz, 1H), 4.49–4.41 (m, 3H), 4.25–4.17 (m, 2H), 4.12–4.07 (m, 1H), 3.93–3.83 (m, 1H), 3.61–3.59 (m, 1H), 3.51–3.46 (m, 1H), 3.27–3.16 (m, 3H), 3.15–3.09 (m, 2H), 2.88–2.76 (m, 2H), 2.62–2.56 (m, 5H), 2.44–2.35 (m, 2H), 2.15–2.07 (m, 2H), 1.95–1.90 (m, 2H), 1.83–1.80 (m, 2H), 1.21 (t, J = 6.0 Hz, 3H). ^{13}C NMR (151 MHz, $CDCl_3$): δ 166.39, 162.80, 162.57, 148.41, 148.10, 137.34, 130.07, 129.92, 129.72, 128.66, 128.25, 126.44, 126.01, 125.93, 125.65, 125.21, 125.05, 118.76, 118.64, 58.99, 58.71, 57.54, 50.32, 41.60, 29.79, 29.71, 29.33, 28.93, 27.22, 26.17, 25.55, 23.40, 22.84, 14.14, 12.40. HR-MS (ESI+) calcd for $C_{35}H_{39}ClN_8O_2H$ $[M+H]^+$ 639.2885 found 639.2946.

5.1.1.7. (E/Z)-2-((S)-4-(7-(8-chloronaphthalen-1-yl)-2-(((S)-1-methylpyrrolidin-2-yl)methoxy)-5,6,7,8-tetrahydropyrido[3,4-d]pyrimidin-4-yl)-2-(cyanomethyl)piperazine-1-carbonyl)-4-methylpent-2-enenitrile (6c). Synthesized according to the method of **6a** using isobutyraldehyde in place of Acetaldehyde to afford product **6c** (15.0 mg, 0.023 mmol, 11% yield) as light brown solid. ^{1}H NMR (400 MHz, $CDCl_3$ mixture of rotamers): δ 7.77 (d, J = 8.0 Hz, 1H), 7.63 (t, J = 8.0 Hz, 1H), 7.54 (d, J = 8.0 Hz, 1H), 7.46 (dd, J_1 = 8.0 Hz, J_2 = 16.0 Hz, 1H), 7.35 (t, J = 8.0 Hz, 1H), 7.24 (dd, J_1 = 8.0 Hz, J_2 = 16.0 Hz, 1H), 7.08 (d, J = 12.0 Hz, 1H), 4.92 (br, 1H), 4.65–4.58 (m, 1H), 4.43 (dd, J_1 = 12.0 Hz, J_2 = 20.0 Hz, 1H), 4.33–4.22 (m, 2H), 4.10 (d, J = 12.0 Hz, 1H), 3.87 (t, J = 20.0 Hz, 1H), 3.63–3.58 (m, 1H), 3.48 (dd, J_1 = 4.0 Hz, J_2 = 16.0 Hz, 1H), 3.36–3.24 (m, 3H), 3.20–3.09 (m, 2H), 3.05–2.96 (m, 3H), 2.86–2.83 (m, 1H), 2.65 (d, J = 12.0 Hz, 3H), 2.61–2.50 (m, 3H), 2.17–2.11 (m, 1H), 2.04–1.96 (m, 1H), 1.91–1.86 (m, 2H), 1.21 (s, 3H), 1.19 (s, 3H). ^{13}C NMR (151 MHz, $CDCl_3$) δ 175.13, 164.71, 164.50, 158.59, 152.67, 149.84, 147.07, 145.46, 138.90, 128.56, 128.36, 127.60, 125.91, 125.72, 124.36, 123.47, 111.85, 100.30, 100.25, 49.95, 49.84, 46.10, 45.12, 43.47, 41.75, 41.58, 39.96, 38.63, 36.44, 27.60, 25.40, 25.36, 22.70, 18.25, 14.14. HR-MS (ESI+) calcd for $C_{36}H_{41}ClN_8O_2H$ $[M+H]^+$ 653.3041 found 653.3093.

5.1.1.8. (E/Z)-2-((S)-4-(7-(8-chloronaphthalen-1-yl)-2-(((S)-1-methylpyrrolidin-2-yl)methoxy)-5,6,7,8-tetrahydropyrido[3,4-d]pyrimidin-4-yl)-2-(cyanomethyl)piperazine-1-carbonyl)-3-cyclopropylacrylonitrile (6d). Synthesized according to the method of **6a** using cyclopropanecarboxaldehyde in place of Acetaldehyde to afford product **6d** (30.0 mg, 27.6% yield) as white solid. ^{1}H NMR (400 MHz, $CDCl_3$ mixture of rotamers): δ 7.77 (d, J = 8.0 Hz, 1H), 7.63 (t, J = 8.0 Hz, 1H), 7.54 (d, J = 8.0 Hz, 1H), 7.49–7.42 (m, 1H), 7.35 (t, J = 8.0 Hz, 1H), 7.24 (dd, J_1 = 8.0 Hz, J_2 = 20.0 Hz, 1H), 6.72 (d, J = 12.0 Hz, 1H), 4.90 (br, 1H), 4.48–4.38 (m, 2H), 4.21–4.06 (m, 2H), 4.07 (d, J = 12.0 Hz, 1H), 3.96–3.82 (m, 1H), 3.62–3.59 (m, 1H), 3.49–3.45 (m, 1H), 3.27–3.17 (m, 2H), 3.16–3.08 (m, 2H), 3.07–3.00 (m, 1H), 2.84 (d, J = 8.0 Hz, 1H), 2.73–2.67 (m, 1H), 2.61–2.56 (m, 1H), 2.50 (d, J = 4.0 Hz, 3H), 2.32–2.28 (m, 1H), 2.15–2.03 (m, 2H), 1.92 (br, 2H), 1.81–1.75 (m, 2H), 0.98–0.97 (m, 1H), 0.91–0.83 (m, 4H). ^{13}C NMR (151 MHz, $CDCl_3$) δ 168.00, 166.36, 166.15, 163.09, 162.59, 148.40, 148.08, 137.31, 130.05, 129.74, 128.30, 126.46, 125.94, 125.68, 125.15, 125.03, 118.57, 115.26, 109.19, 69.42, 64.12, 59.03, 58.73, 57.60, 50.28, 47.77, 47.36, 41.64, 28.94, 26.92, 26.23, 25.67, 22.88, 16.12, 11.23. HR-MS (ESI+) calcd for $C_{36}H_{39}ClN_8O_2H$ $[M+H]^+$ 651.2885, found 651.2932.

5.1.1.9. (E/Z)-2-((S)-4-(7-(8-chloronaphthalen-1-yl)-2-(((S)-1-methylpyrrolidin-2-yl)methoxy)-5,6,7,8-tetrahydropyrido[3,4-d]pyrimidin-4-yl)-2-(cyanomethyl)piperazine-1-carbonyl)-4,4-dimethylpent-2-enenitrile (6e). To a solution of compound **11** (100.0 mg, 0.17 mmol, 1.0 eq.) and pivaldehyde (21.6 mg, 1.5 eq.) in EtOH (5.0 mL) was added TEA (33.8 mg, 2.0 eq.) and the mixture

was stirred at 65 °C for 16 h under N_2 atmosphere. The reaction mixture was purified by column chromatography (SiO_2, DCM/MeOH = 20:0 to 20:1) to afford product **6e** (12.0 mg, 11% yield) as gray solid. ^{1}H NMR (400 MHz, $CDCl_3$ mixture of rotamers): δ 7.77 (d, J = 8.0 Hz, 1H), 7.63 (t, J = 8.0 Hz, 1H), 7.54 (d, J = 8.0 Hz, 1H), 7.49–7.43 (m, 1H), 7.35 (t, J = 4.0 Hz, 1H), 7.24 (dd, J_1 = 4.0 Hz, J_2 = 20.0 Hz, 1H), 7.10 (s, 1H), 4.97 (br, 1H), 4.47–4.40 (m, 2H), 4.23–4.18 (m, 2H), 4.08 (d, J = 8 Hz, 1H), 3.95 (d, J = 8.0 Hz, 1H), 3.93–3.83 (m, 1H), 3.61–3.58 (m, 1H), 3.47 (J_1 = 4.0 Hz, J_2 = 12.0 Hz, 1H), 3.26 (d, J = 8.0 Hz, 1H), 3.19–3.12 (m, 3H), 2.82–2.77 (m, 2H), 2.59 (d, J = 8.0 Hz, 1H), 2.54 (d, J = 8.0 Hz, 3H), 2.37–2.35 (m, 2H), 2.11–2.07 (m, 2H), 1.90–1.87 (m, 1H), 1.82–1.79 (m, 2H), 1.34 (s, 9H). ^{13}C NMR (151 MHz, $CDCl_3$) δ 166.36, 166.23, 163.91, 163.82, 162.62, 148.42, 148.10, 137.34, 130.07, 129.72, 128.24, 126.43, 126.01, 125.94, 125.65, 125.16, 125.03, 118.75, 118.64, 69.48, 64.19, 58.97, 58.69, 57.55, 50.38, 47.70, 47.31, 41.61, 35.62, 29.71, 29.01, 26.92, 26.17, 22.88, 14.14. HR-MS (ESI+) calcd for $C_{37}H_{43}ClN_8O_2H$ $[M+H]^+$ 667.3198 found 667.3246.

5.1.2. Synthesis of PROTAC YF135

5.1.2.1. tert-butyl 4-hydroxy-2-(methylthio)-5,8-dihydropyrido[3,4-d]pyrimidine-7(6H)-carboxylate (13). To a stirred solution of 1-*tert*-butyl 4-ethyl 3-oxopiperidine-1,4-dicarboxylate **12** (10.0 g, 36.8 mmol, 1.0 eq.) in MeOH (300 mL) was added MeONa (10.0 g, 5.0 eq.) and 2-methyl-2-thiopseudourea sulfate (18.5 g, 1.8 eq.). The reaction mixture was acidified with HCl (2 M) until pH~5 after stirred at rt overnight. and then concentrated under reduced pressure to removed MeOH. The residue was resuspended in 100 mL of ethyl acetate and 100 mL of water and stirred rapidly. The filtrate was collected and washed with water (3x30 mL), dried in vacuo to obtained as a white solid (7.0 g, 64.2% yield) and used directly for next step without further purification. ESI-MS m/z: 298.1 $[M+H]^+$.

5.1.2.2. tert-butyl 2-(methylthio)-4-(((trifluoromethyl)sulfonyl)oxy)-5,8-dihydropyrido[3,4-d]pyrimidine-7(6H)-carboxylate (14). To a stirred suspension of **13** (7.0 g, 16.8 mmol, 1.0 eq.) in DCM (250 mL) at 0 °C was added DIPEA (4.4 g, 2.0 eq.) followed by Tf_2O (6.2 g, 1.3 eq.) under nitrogen. After stirring at rt for 16 h, the reaction was concentrated to give a brown oil. The brown oil was purified by column chromatography (SiO_2, PE/EA = 1:0 to 10:1) to give the title compound (4.5 g, 44.5% yield) as a yellow solid. ESI-MS m/z: 430.1 $[M+H]^+$.

5.1.2.3. tert-butyl (S)-4-(4-((benzyloxy)carbonyl)-3-(cyanomethyl) piperazin-1-yl)-2-(methylthio)-5,8-dihydropyrido[3,4-d]pyrimidine-7(6H)-carboxylate (16). A mixture of **14** (3.2 g, 7.5 mmol, 1.0 eq.), benzyl-(*2S*)-2-(cyanomethyl)piperazine-1-carboxylate **15** (1.9 g, 1.0 eq.), and DIPEA (2.9 g, 3.0 eq) in MeCN (25 mL) was stirred at 100 °C under N_2 atmosphere. The solvent was removed under vacuum after TLC showed the complete consumption of **14**, The residue was purified by column chromatography (SiO_2, PE/EA = 3:1 to 1:1) to give title compound (3.2 g, 80% yield) as a yellow solid. ^{1}H NMR (400 MHz, $CDCl_3$) δ 7.43–7.35 (m, 5H), 5.21 (s, 2H), 4.69 (s, 2H), 4.63 (d, J = 20.0 Hz, 1H), 4.39 (d, J = 20.0 Hz, 1H), 4.16–4.10 (m, 1H), 3.99 (d, J = 16.0 Hz, 1H), 3.89–3.79 (m, 2H), 3.4–3.3 (m, 3H), 3.02 (td J_1 = 4.0 Hz, J_2 = 12.0 Hz, 1H), 2.78–2.60 (m, 4H), 2.52 (s, 3H), 1.51 (s, 9H). ESI-MS m/z: 539.2 $[M+H]^+$.

5.1.2.4. benzyl (S)-4-(7-(8-chloronaphthalen-1-yl)-2-(methylthio)-5,6,7,8-tetrahydropyrido[3,4-d]pyrimidin-4-yl)-2-(cyanomethyl) piperazine-1-carboxylate (17). To a solution of **16** (3.2 g, 5.9 mmol, 1.0 eq.) in DCM (25 mL), was added TFA (10 mL) and the mixture was stirred at rt for 3 h. After completion, the reaction mixture was quenched with saturated $NaHCO_3$ solution, extracted with DCM (3x50 mL) and the organic layer was dried under vacuum to give a yellow solid (2.5 g, yield 96%) which was used for the next step immediately without further purification.

To a solution of above product (2.5 g, 5.6 mmol, 1.0 eq.), 1-bromo-8-chloro-naphthalene (2.5 g, 1.8 eq.), $Pd_2(dba)_3$ (540 mg, 0.1 eq.), XantPhos (680 mg, 0.2 eq.) and Cs_2CO_3 (7.0 g, 3.6 eq.) in toluene (30 mL) was degassed and purged with N_2 3 times, and then the mixture was stirred at 100 °C for 18 h under N_2 atmosphere. The reaction mixture was filtered and solvent was removed under vacuum to give an oil residue. The residue was purified by column chromatography (SiO_2, PE/EA = 5:1 to 3:1) to give the title compound (2.1 g, 59% yield) as a brown solid.

^{1}H NMR (400 MHz, $CDCl_3$) δ 7.77 (d, J = 8.0 Hz, 1H), 7.63 (t, J = 8.0 Hz, 1H), 7.54 (d, J = 4.0 Hz, 1H), 7.47 (t, J = 5.0 Hz, 1H), 7.46–7.38 (m, 5H), 7.35 (t, J = 8.0 Hz, 1H), 7.24 (dd, J_1 = 8.0 Hz, J_2 = 16.0 Hz, 1H), 5.22 (s, 2H), 4.71 (s, 1H), 4.46 (dd, J_1 = 12.0 Hz, J_2 = 20.0 Hz, 1H), 4.17–4.03 (m, 2H), 3.99–3.95 (m, 1H), 3.86 (t, J = 20.0 Hz, 1H), 3.61–3.58 (m, 1H), 3.42 (d, J = 12 Hz, 1H), 3.32–3.09 (m, 3H), 3.04–2.92 (m, 1H), 2.84–2.70 (m, 2H), 2.59 (t, J = 12.0 Hz, 1H), 2.52 (d, J = 4.0 Hz, 3H). ESI-MS m/z: 599.2 $[M+H]^+$.

5.1.2.5. benzyl (S)-4-(2-(((S)-1-(3-(3-(tert-butoxy)-3-oxopropoxy) propyl)pyrrolidin-2-yl)methoxy)-7-(8-chloronaphthalen-1-yl)-5,6,7,8-tetrahydropyrido[3,4-d]pyrimidin-4-yl)-2-(cyanomethyl) piperazine-1-carboxylate (19). To a solution of **17** (734 mg, 1.0 eq) in DCM, was addend *m*-CPBA (1.2 eq.) in portions and the reaction stirred at rt overnight. The reaction was quenched with water (20 mL) and extracted with DCM (3x10 mL). The combined organic layer was dried over Na_2SO_4, and purified by column chromatography (SiO_2, Methanol/Ethyl acetate = 0:1 to 1:10) to give the title compound (350 mg, 46% yield) as a yellow solid.

To a mixture of above product (400 mg, 65 mmol, 1.0 eq.) and **18** (560.0 mg, 3.0 eq.) in toluene (5 mL) was added *t*-BuONa (187.0 mg, 3.0 eq.). The mixture was stirred at room temperature for 2 h. Added to cold water (5 mL) and extracted with ethyl acetate (3x5 mL) after completion, then, concentrated and purified by column chromatography (SiO_2, DCM/MeOH = 100:0 to 100:3) to give the title compound (120 mg, 22% yield) as a yellow solid. ^{1}H NMR (400 MHz, $CDCl_3$) δ 7.77 (d, J = 8.0 Hz, 1H), 7.62 (t, J = 10.0 Hz, 1H), 7.53 (d, J = 4.0 Hz, 1H), 7.46 (dd, J_1 = 8.0 Hz, J_2 = 16.0 Hz, 1H), 7.41–7.38 (m, 5H), 7.35 (t, J = 8.0 Hz, 1H), 7.24 (m, 1H), 5.22 (s, 2H), 4.70 (s, 1H), 4.43 (t, J = 16.0 Hz, 1H), 4.38–4.34 (m, 1H), 4.19–4.04 (m, 3H), 3.99–3.94 (m, 1H), 3.87–3.80 (m, 1H), 3.71–3.65 (m, 2H), 3.64–3.58 (m, 2H), 3.51–3.47 (m, 2H), 3.42–3.37 (m, 1H), 3.27–3.06 (m, 4H), 3.03–2.80 (m, 4H), 2.80–2.71 (m, 1H), 2.59 (d, J = 12.0 Hz, 1H), 2.50 (t, J = 6.0 Hz, 1H), 2.45 (t, J = 8.0 Hz, 2H), 2.27–2.22 (m, 1H), 2.04–1.99 (m, 1H), 1.82–1.76 (m, 4H), 1.44 (s, 9H). ESI-MS m/z: 838.4 $[M+H]^+$.

5.1.3. tert-butyl 3-(3-((S)-2-(((7-(8-chloronaphthalen-1-yl)-4-((S)-3-(cyanomethyl)piperazin-1-yl)-5,6,7,8-tetrahydropyrido[3,4-d] pyrimidin-2-yl)oxy)methyl)pyrrolidin-1-yl)propoxy)propanoate (20)

To a solution of **19** (180 mg, 1.0 eq.) in MeOH (20 mL) was added DCM (3 mL) and Pd/C (100 mg, 10% purity), The suspension was degassed under vacuum and purged with H_2 several times. The mixture was stirred at room temperature for 36h. Upon completion, the catalyst was filtered off and the filtrate was concentrated under vacuum to give the title compound (100 mg, 52% yield) as a yellow solid which was used directly in the next step without further purification. ESI-MS m/z: 704.3 $[M+H]^+$.

5.1.3.1. (E/Z)-2-cyano-3-cyclopropylacryloyl cyanide (18). To a suspension of 2-cyanoacetic acid (1.3 g, 15.3 mmol, 1.0 eq.) in toluene (5.0 mL) was added cyclopropanecarbaldehyde (1.07 g, 1.0 eq.) and

Ammonium acetate (250.0 mg, 0.25 eq.), The mixture was stirred at 110 °C for 1h, then, cool down to room temperature, the precipitate was filtered and dried in vacuo to gives title compound (800.0 mg, 40% yield) as white solid. ^{1}H NMR (400 MHz, DMSO-d_6) δ 7.31 (s, 1H), 6.96 (s, 0.5H), 6.93 (s, 0.5H), 1.86 (m, 1H), 1.19 (m, 2H), 0.94 (m, 2H). ESI-MS *m/z*: 135.8 $[M - H]^-$.

5.1.3.2. tert-butyl 3-(3-((S)-2-(((7-(8-chloronaphthalen-1-yl)-4-((S)-4-((Z)-2-cyano-3-cyclopropylacryloyl)-3-(cyanomethyl)piperazin-1-yl)-5,6,7,8-tetrahydropyrido[3,4-d]pyrimidin-2-yl)oxy)methyl)pyrrolidin-1-yl)propoxy)propanoate (22). To a solution of **20** (100 mg, 0.14 mmol, 1.0 eq.) in DCM (15.0 mL) was added **18** (30.0 mg, 1.5 eq.), HATU (80.0 mg, 1.5 eq.), and TEA (43.0 mg, 3.0 eq.). The mixture was stirred at room temperature for 3.5 h. After completion, the residue was diluted with H_2O (5 mL), extracted with DCM (25 mL X 2), concentrated under vacuum and purified by column chromatography (SiO_2, DCM/MeOH = 100:0 to 100:5) to give the title compound (32.0 mg, 27.4 yield%) as solid. HR-MS $C_{45}H_{55}ClN_8O_5$ $[M+H]^+$: 823.3984 found 823.4037.

5.1.3.3. (2S,4R)-1-((S)-2-(3-(3-((S)-2-(((7-(8-chloronaphthalen-1-yl)-4-((S)-4-((Z/E)-2-cyano-3-cyclopropylacryloyl)-3-(cyanomethyl) piperazin-1-yl)-5,6,7,8-tetrahydropyrido[3,4-d]pyrimidin-2-yl)oxy) methyl)pyrrolidin-1-yl)propoxy)propanamido)-3,3-dimethylbutanoyl)-4-hydroxy-N-(4-(4-methylthiazol-5-yl)benzyl) pyrrolidine-2-carboxamide (YF135). To a solution of **22** (32.0 mg, 1.0 eq.) in DCM (1 mL) was added TFA (1.0 mL), and the mixture was stirred for 0.5 h at room temperature, concentrated under vacuum and used in the next step without further purification.

To a solution of above product (1.0 eq.) in DMF (1 mL) was added VHL ligand (Following a literature procedure [33].) (1.2 eq.), HATU (1.3 eq.), and TEA (5.0 eq.). The mixture was stirred for 2 h at room temperature. Upon completion, the mixture was diluted with H_2O (5 mL), extracted with EtOAc (5.0 mL X 3), dried over Na_2SO_4, concentrated under vacuum and purified by column chromatography (SiO_2, DCM/MeOH = 100:0 to 100:5) to give the title compound (10 mg, 22.2% for two steps) as gray solid. ^{1}H NMR (400 MHz, Acetone-d_6) δ 8.85 (s, 1H), 7.90 (d, J = 8.0 Hz, 1H), 7.73 (d, J = 8.0 Hz, 1H), 7.58 (d, J = 8.0 Hz, 1H), 7.52 (t, J = 8.0 Hz, 2H), 7.49–7.46 (m, 3H), 7.42 (dd, J_1 = 4.0 Hz, J_2 = 8.0 Hz, 1H), 7.38–7.36 (m, 3H), 6.67 (t, J = 10 Hz, 1H), 4.97 (s, 1H), 4.68 (d, J = 8.0 Hz, 2H), 4.52 (s, 3H), 4.40–4.33 (m, 2H), 4.31 (d, J = 12.0 Hz, 1H), 4.25–4.17 (m, 2H), 4.09 (d, J = 12.0 Hz, 1H), 3.90–3.81 (m, 2H), 3.79–3.73 (m, 2H), 3.67–3.63 (m, 2H), 3.61–3.59 (m, 1H), 3.58–3.45 (m, 5H), 3.36–3.17 (m, 5H), 3.14–3.08 (m, 5H), 2.46 (s, 3H), 2.23–2.10 (m, 3H), 1.35 (t, J = 8.0 Hz, 6H), 1.32–1.30 (m, 3H), 1.28–1.25 (m, 2H), 1.00 (d, J = 2.4 Hz, 9H). ^{13}C NMR (150 MHz, Acetone-d_6) δ 171.94, 170.29, 165.23, 165.14, 164.40, 162.90, 150.41, 148.59, 148.14, 139.74, 137.54, 131.46, 130.22, 128.88, 128.85, 128.54, 128.49, 127.74, 127.70, 126.83, 125.80, 125.70, 125.01, 119.07, 118.91, 117.54, 115.19, 115.06, 106.80, 69.71, 66.75, 59.11, 59.03, 58.86, 56.81, 56.73, 56.67, 50.24, 50.16, 45.24, 42.06, 37.82, 36.42, 35.52, 35.48, 31.77, 30.79, 29.51, 26.89, 26.06, 22.47, 15.53, 15.30, 13.53, 9.60, 7.91. HR-MS $C_{63}H_{75}ClN_{12}O_7S$ $[M+H]^+$ = 1179.5291 found 1179.5346.

5.2. Biological

5.2.1. $KRAS^{G12C}$ HTRF assay (Testing services by Shanghai WuXi PharmaTech)

The HTRF $KRAS^{G12C}$/SOS1 Binding Assay is designed to measure the interaction between $KRAS^{G12C}$ and SOS1 proteins by using HTRF (Homogeneous Time-resolved Fluorescence) technology. In brief, the interaction between SOS1 and $KRAS^{G12C}$ is detected by using Tag1-Terbium (HTRF donor) and Tag2-XL665 (HTRF acceptor). When the donor and acceptor get close proximity due to SOS1 and $KRAS^{G12C}$ binding, excitation of the donor triggers fluorescent resonance energy transfer (FRET) towards the acceptor, which in turn emits specifically at 665 nm. This specific signal is directly proportional to the extent of $KRAS^{G12C}$/SOS1 interaction.

5.2.2. CCK-8 assay

H358, A549 and H23 cells were purchased from the Shanghai cell library. These cells were cultured in RPMI Medium 1640 supplemented with 10% fetal bovine serum, 100 U/mL penicillin and 100 mg/mL streptomycin with 5% CO_2 at 37 °C in a humidified incubator. Counting Kit-8 (CCK-8) from MedChemExpress (Madison, WI, USA) was used to measure the proliferation of H358, H23 and A549 cells. Cells (1000 cells/well) were seeded in 96-well plates and exposed to compounds at various concentrations. 72 h later, CCK-8 solution was added to each well, and incubated at 37 °C for 60 min. Cell viability was determined by measuring the absorbance at 450 nm.

5.2.3. Western blotting

Cells were lysed with NETN buffer (20 mM Tris-HCl, pH 8.0, 100 mM NaCl, 1 mM EDTA, 0.5% Nonidet P-40) containing 50 mM β-glycerophosphate, 10 mM NaF, and 1 mg/ml each of pepstatin A and aprotinin. Protein concentrations were determined by BCA protein assay kit (Thermo scientific). An equal amount of proteins was loaded onto an SDS-PAGE gel, and electrophoretic separation was performed at a constant voltage of 100 V. The separated proteins were then transferred to PVDF membrane (Millipore) at a constant current of 280 amps. The membrane was blocked with 5% w/v skim milk for 1 h at room temperature. The membrane was then incubated in solutions containing either KRAS antibody (Abcam), p-ERK antibody (Cell Signaling), total ERK antibody (Cell Signaling) or β-actin antibody (Sigma-Aldrich) at 4 °C overnight. Goat Anti-Rabbit IgG (H + L) (1:1000 dilution; Thermo Scientific) coupled with the corresponding horseradish peroxidase (HRP) was incubated with ECL Western Blotting Substrate Kit (Perkin Elmer) to observe protein bands. Use Image J software (National Institutes of Health, National Institutes of Health) to quantify the bands and normalize the target protein level to β-actin.

5.2.4. Washout assay

Cells were treated with vehicle or YF135 for 24hs and three times of washout by fresh medium was performed at different time points (8, 12 and 16hrs). Cell pellets were collected and western blotting was performed with indicated antibodies. For washout assay in the presence of cycloheximide, H358 cells were treated with vehicle or YF135 for 12 h and three times of washout by fresh medium were performed at 12h. Then cells were treated with vehicle or cycloheximide (MCE) for 8 h. Cell pellets were collected and western blotting was performed with indicated antibodies.

5.2.5. Expression and purification of the $KRAS^{G12C}$ protein

DNA sequence encoding $KRAS^{G12C}$ was inserted into a modified pET28a vector, in which the $KRAS^{G12C}$ gene was separated from an N-terminal His_6-thioredoxin tag by a TEV cleavage site. The plasmid was transformed into BL21(DE3) cells. The expression of proteins was induced by isopropyl β-D-1-thiogalactopyranoside (IPTG) when the cell density reached an OD_{600} of 1.0. The bacterial continued to grow at 16 °C overnight. The recombinant proteins were purified through a Nickel Affinity column, and the His_6-thioredoxin tag was subsequently removed by TEV cleavage and anion exchange chromatography (Hitrap Q, GE Healthcare). Fractions containing $KRAS^{G12C}$ were loaded on a Superdex 75 column (GE Healthcare) equilibrated with 25 mM Tris (pH 8.0) and 100 mM NaCl. The proteins were finally concentrated to 33 mg/mL and stored at −80 °C for further use [34].

6. MALDI-TOF-MS

6.1. Method

Matrix-assisted laser desorption/ionization time-of-flight mass spectrometry (MALDI-TOF-MS) was preformed to determine the molecular weight of samples. Sinapic acid (Sigma Part No #85429, USA) was used as the matrix on the apparatus (Bruker UltrafleXtreme, Germany). Linear positive ion mode, contained the suitable detection range of molecular weight, was selected as the detection method. Desalting samples (<1 mg/mL) were mixed with matrix solution (20 mg/ml, 50% water and 50% acetonitrile) at a volume ratio of 1:1. The Mass spectrogram was worked in FlexAnalysis and Origin [35].

6.2. MALDI-TOF-MS for 6d

$KRAS^{G12C}$ protein (400 nM) was mixed with the **6d** (4 μM) in a molar ratio of 1:10 in 1 mL protein assay buffer (40 mM Tris-HCl pH 7.5, 20 mM MgCl2, 20 mM NaCl, 0.1 mg/mL BSA, 1 mM TCEP, and 4% DMSO) for 2hrs at room temperature. Then half of protein/inhibitor mixture was stored at 4 °C, while another half of protein/inhibitor mixture was transferred to a dialysis cassette (1 mL, 3 kDa MWCO, Spectra/Por Part No #0290030, USA) and dialyzed in 1L buffer at 4 °C. The protein/inhibitor complex was dialyzed in water for one day and concentrated. Both samples were then subjected to MALDI-TOF-MS.

7. Molecular modeling

The protein structure of KRAS was downloaded from PDB data bank (PDB ID: 6UT0) and prepared by Protein Preparation Wizard (Schrödinger, LLC, New York, NY, 2019). The compound **6d** was prepared by Ligprep. CovDock [36] was applied for covalent docking using default settings. To model the ternary structure for KRAS, VHL and YF135, we followed the protocol as described in previous works with some modifications [37,38]. In brief, protein-protein docking was performed by using Rosetta. ConfGen was employed to generate conformers. The low energy linkers were aligned to the favorable docking pose to built the ternary structure.

Declaration of competing interest

The authors declare that they have no known competing financial interests or personal relationships that could have appeared to influence the work reported in this paper.

Acknowledgements

We appreciate the financial support from National Natural Science Foundation of China (81922062 XL, 81874285 XL and 81773758 TL), Science and Technology Planning Project of Guangzhou City (201804010493 TL), the Natural Science Foundation of Guangdong Province (2019A1515011934 and 2021A1515011233 TL), K. C. Wong Education Foundation and the High-Performance Public Computing Service Platform of Jinan University.

Appendix A. Supplementary data

Supplementary data related to this article can be found at https://doi.org/10.1016/j.ejmech.2021.114088.

References

[1] K. Scheffzek, M.R. Ahmadian, W. Kabsch, L. Wiesmüller, A. Lautwein, F. Schmitz, A. Wittinghofer, The Ras-RasGAP complex: structural basis for GTPase activation and its loss in oncogenic Ras mutants, Science 277 (1997) 333–339.
[2] A.D. Cox, C.J. Der, Ras history: the saga continues, Small GTPases 1 (2010) 2–27.
[3] J.C. Hunter, A. Manandhar, M.A. Carrasco, D. Gurbani, S. Gondi, K.D. Westover, Biochemical and structural analysis of common cancer-associated KRAS mutations, Mol. Cancer Res. 13 (2015) 1325–1335.
[4] C. Muñoz-Maldonado, Y. Zimmer, M. Medová, A comparative analysis of individual RAS mutations in cancer biology, Front. Oncol. 9 (2019) 1088–1109.
[5] I.A. Prior, P.D. Lewis, C. Mattos, A comprehensive survey of Ras mutations in cancer, Cancer Res. 72 (2012) 2457–2467.
[6] D.K. Simanshu, D.V. Nissley, F. McCormick, RAS proteins and their regulators in human disease, Cell 170 (2017) 17–33.
[7] J.M. Ostrem, U. Peters, M.L. Sos, J.A. Wells, K.M. Shokat, K-Ras (G12C) inhibitors allosterically control GTP affinity and effector interactions, Nature 503 (2013) 548–551.
[8] F. McCormick, KRAS as a therapeutic target, Clin. Cancer Res. 21 (2015) 1797–1801.
[9] D. Uprety, A.A. Adjei, KRAS: from undruggable to a druggable Cancer Target, Cancer Treat Rev. 89 (2020) 102070–102083.
[10] A. Matikas, D. Mistriotis, V. Georgoulias, A. Kotsakis, Targeting KRAS mutated non-small cell lung cancer: a history of failures and a future of hope for a diverse entity, Crit. Rev. Oncol.-Hematol. 110 (2017) 1–12.
[11] H. Chen, J.B. Smaill, T. Liu, K. Ding, X. Lu, Small-molecule inhibitors directly targeting KRAS as anticancer therapeutics, J. Med. Chem. 63 (2020) 14404–14424.
[12] M.R. Janes, J. Zhang, L.-S. Li, R. Hansen, U. Peters, X. Guo, Y. Chen, A. Babbar, S.J. Firdaus, L. Darjania, Targeting KRAS mutant cancers with a covalent G12C-specific inhibitor, Cell 172 (2018) 578–589, e517.
[13] J. Canon, K. Rex, A.Y. Saiki, C. Mohr, K. Cooke, D. Bagal, K. Gaida, T. Holt, C.G. Knutson, N. Koppada, The clinical KRAS (G12C) inhibitor AMG 510 drives anti-tumour immunity, Nature 575 (2019) 217–223.
[14] B.A. Lanman, J.R. Allen, J.G. Allen, A.K. Amegadzie, V.J. Cee, Discovery of a covalent inhibitor of KRASG12C (AMG 510) for the treatment of solid tumors, J. Med. Chem. 63 (2020) 52–65.
[15] J. Hallin, L.D. Engstrom, L. Hargis, A. Calinisan, R. Aranda, D.M. Briere, N. Sudhakar, V. Bowcut, B.R. Baer, J.A. Ballard, The KRASG12C inhibitor MRTX849 provides insight toward therapeutic susceptibility of KRAS-mutant cancers in mouse models and patients, Cancer Discov. 10 (2020) 54–71.
[16] J.B. Fell, J.P. Fischer, B.R. Baer, J.F. Blake, K. Bouhana, D.M. Briere, K.D. Brown, L.E. Burgess, A.C. Burns, M.R. Burkard, Identification of the clinical development candidate MRTX849, a covalent KRASG12C inhibitor for the treatment of cancer, J. Med. Chem. 63 (2020) 6679–6693.
[17] M.M. Awad, S. Liu, I.I. Rybkin, K.C. Arbour, J. Dilly, V.W. Zhu, M.L. Johnson, R.S. Heist, T. Patil, G.J. Riely, Acquired resistance to KRASG12C inhibition in cancer, N. Engl. J. Med. 384 (2021) 2382–2393.
[18] N.S. Akhave, A.B. Biter, D.S. Hong, Mechanisms of resistance to KRASG12C-targeted therapy, Cancer Discov. 11 (2021) 1345–1352.
[19] D.P. Bondeson, A. Mares, I.E. Smith, E. Ko, S. Campos, A.H. Miah, K.E. Mulholland, N. Routly, D.L. Buckley, J.L. Gustafson, Catalytic in vivo protein knockdown by small-molecule PROTACs, Nat. Chem. Biol. 11 (2015) 611–617.
[20] A.C. Lai, C.M. Crews, Induced protein degradation: an emerging drug discovery paradigm, Nat. Rev. Drug Discov. 16 (2017) 101–114.
[21] M. Zeng, Y. Xiong, N. Safaee, R.P. Nowak, K.A. Donovan, C.J. Yuan, B. Nabet, T.W. Gero, F. Feru, L. Li, Exploring targeted degradation strategy for oncogenic KRASG12C, Cell Chem. Biol. 27 (2020) 19–31, e16.
[22] M.J. Bond, L. Chu, D.A. Nalawansha, K. Li, C.M. Crews, Targeted degradation of oncogenic KRASG12C by VHL-recruiting PROTACs, ACS Cent. Sci. 6 (2020) 1367–1375.
[23] R.B. Kargbo, PROTAC-mediated degradation of KRAS protein for anticancer therapeutics, ACS Med. Chem. Lett. 11 (2020) 5–6.
[24] R. Gabizon, A. Shraga, P. Gehrtz, E. Livnah, Y. Shorer, N. Gurwicz, L. Avram, T. Unger, H. Aharoni, S. Albeck, Efficient targeted degradation via reversible and irreversible covalent PROTACs, J. Am. Chem. Soc. 142 (2020) 11734–11742.
[25] H. Kiely-Collins, G.E. Winter, G.J. Bernardes, The role of reversible and irreversible covalent chemistry in targeted protein degradation, Cell Chem. Biol. 28 (2021) 952–968.
[26] C.P. Tinworth, H. Lithgow, L. Dittus, Z.I. Bassi, S.E. Hughes, M. Muelbaier, H. Dai, I.E. Smith, W.J. Kerr, G.A. Burley, PROTAC-mediated degradation of Bruton's tyrosine kinase is inhibited by covalent binding, ACS Chem. Biol. 14 (2019) 342–347.
[27] W.-H. Guo, X. Qi, X. Yu, Y. Liu, C.-I. Chung, F. Bai, X. Lin, D. Lu, L. Wang, J. Chen, Enhancing intracellular accumulation and target engagement of PROTACs with reversible covalent chemistry, Nat. Commun. 11 (2020) 1–16.
[28] A. Bandyopadhyay, J. Gao, Targeting biomolecules with reversible covalent chemistry, Curr. Opin. Chem. Biol. 34 (2016) 110–116.
[29] M. Forster, A. Chaikuad, S.M. Bauer, J. Holstein, M.B. Robers, C.R. Corona, M. Gehringer, E. Pfaffenrot, K. Ghoreschi, S. Knapp, Selective JAK3 inhibitors

with a covalent reversible binding mode targeting a new induced fit binding pocket, Cell Chem. Biol. 23 (2016) 1335–1340.
[30] C. Ambrogio, J. Köhler, Z.-W. Zhou, H. Wang, R. Paranal, J. Li, M. Capelletti, C. Caffarra, S. Li, Q. Lv, KRAS dimerization impacts MEK inhibitor sensitivity and oncogenic activity of mutant KRAS, Cell 172 (2018) 857–868, e815.
[31] L.-R. Zeng, M.E. Vega-Sánchez, T. Zhu, G.-L. Wang, Ubiquitination-mediated protein degradation and modification: an emerging theme in plant-microbe interactions, Cell Res. 16 (2006) 413–426.
[32] X. Zhang, F. Xu, L. Tong, T. Zhang, H. Xie, X. Lu, X. Ren, K. Ding, Design and synthesis of selective degraders of EGFRL858R/T790M mutant, Eur. J. Med. Chem. 192 (2020) 112199.
[33] X. Han, C. Wang, C. Qin, W. Xiang, E. Fernandez-Salas, C.-Y. Yang, M. Wang, L. Zhao, T. Xu, K. Chinnaswamy, Discovery of ARD-69 as a highly potent proteolysis targeting chimera (PROTAC) degrader of androgen receptor (AR) for the treatment of prostate cancer, J. Med. Chem. 62 (2019) 941–964.
[34] A.K. Bera, J. Lu, T.E. Wales, S. Gondi, D. Gurbani, A. Nelson, J.R. Engen, K.D. Westover, Structural basis of the atypical activation mechanism of KRASV14I, J. Biol. Chem. 294 (2019) 13964–13972.
[35] Z. Zhou, X. Chen, Y. Fu, Y. Zhang, S. Dai, J. Li, L. Chen, G. Xu, Z. Chen, Y. Chen, Characterization of FGF401 as a reversible covalent inhibitor of fibroblast growth factor receptor 4, Chem. Commun. 55 (2019) 5890–5893.
[36] K. Zhu, K.W. Borrelli, J.R. Greenwood, T. Day, R. Abel, R.S. Farid, E. Harder, Docking covalent inhibitors: a parameter free approach to pose prediction and scoring, J. Chem. Inf. Model. 54 (2014) 1932–1940.
[37] G. Luo, Z. Li, X. Lin, X. Li, Y. Chen, K. Xi, M. Xiao, H. Wei, L. Zhu, H. Xiang, Discovery of an orally active VHL-recruiting PROTAC that achieves robust HMGCR degradation and potent hypolipidemic activity in vivo, Acta Pharm. Sin. B 11 (2021) 1300–1314.
[38] N. Bai, S.A. Miller, G.V. Andrianov, M. Yates, P. Kirubakaran, J. Karanicolas, Rationalizing PROTAC-mediated ternary complex formation using Rosetta, J. Chem. Inf. Model. 61 (2021) 1368–1382.